Synthesis of molecularly printed methyl methacrylate--based polymers for the detection of di(2-ethylhexyl) phthalate and dibutyl phthalate

St Fauziah[1), *)] (ORCID ID: 0000-0002-0599-4011), **Nunuk Hariani Soekamto**[1)] (0000-0001-8281-1752), **Prastawa Budi**[1)] (0000-0002-1266-5232), **Herlina Rasyid**[1)] (0000-0001-9136-9716), **Nur Haedar**[2)] (0000-0002-6200-298X), **Muraalia Hustim**[3)] (0000-0001-8323-1549), **Marlina Marlina**[1)] (0009-0008-0629-7614), **Magfirah Sulaiman**[1)] (0009-0009-5156-7844), **Ajuk Sapar**[4)] (0000-0002-7278-6159)

DOI: https://doi.org/10.14314/polimery.2022.7.7

Abstract: Molecularly imprinted polymers (MIP) were obtained by precipitation polymerization for the detection of DEHP and DBP from polymer packaging in drinking water. MIP was obtained by cross-linking DEHP and DBP with methyl methacrylate (MMA) and trimethylolpropane trimethacrylate (TRIM). FTIR, SEM-EDS, UV-Vis and SAA were used to determine properties of polymers (MIP_DEHP, MIP_DBP). The obtained materials were characterized by a mesoporous structure with small, uniform, and porous grains. The surface area and total pore volume of MIP_DEHP were more than twice smaller than MIP_DBP, with a slightly larger pore diameter. Lower C content may indicate the formation of MIP_DEHP and MIP_DBP. The FTIR method confirmed the presence of functional groups –CH, –CO, –C=C and –C=O. The adsorption capacity of MIP_DEHP and MIP_DBP was 0.68 mg/g and 1.06 mg/g, respectively, and was consistent with the Freundlich isothermal adsorption model.

Keywords: molecularly imprinted polymers, phthalates, methyl methacrylate, trimethylolpropane trimethacrylate.

Synteza polimerów na bazie metakrylanu metylu z nadrukiem molekularnym do wykrywania ftalanu di(2-etyloheksylu) i ftalanu dibutylu

Streszczenie: Metodą polimeryzacji strąceniowej otrzymano polimery z nadrukiem molekularnym (MIP) do wykrywania DEHP i DBP z opakowań polimerowych w wodzie pitnej. MIP otrzymano poprzez sieciowanie DEHP i DBP metakrylanem metylu (MMA) i trimetakrylanem trimetylolopropanu (TRIM). Do oceny właściwości polimerów (MIP_DEHP, MIP_DBP) zastosowano FTIR, SEM-EDS, UV-Vis i SAA. Otrzymane materiały charakteryzowały się mezoporowatą strukturą o małych, jednolitych i porowatych ziarnach. Pole powierzchni i całkowita objętość porów MIP_DEHP były ponad dwukrotnie mniejsze niż MIP_DBP, przy nieznacznie większej średnicy porów. Mniejsza zawartość C może świadczyć o tworzeniu się MIP_DEHP i MIP_DBP. Metodą FTIR potwierdzono obecność grup funkcyjnych -CH, –CO, –C=C i –C=O. Zdolność adsorpcyjna MIP_DEHP i MIP_DBP wynosiła odpowiednio 0,68 mg/g i 1,06 mg/g i była zgodna z izotermicznym modelem adsorpcji Freundlicha.

Słowa kluczowe: polimery z nadrukiem molekularnym, ftalany, metakrylan metylu, trimetakrylan trimetylolopropanu.

Polymers are widely used in food packaging and children's accessories because they are flexible, strong, transparent, waterproof, and cheap [1]. However, they contain additives such as plasticizers that may affect human health [2]. For example, polyethylene terephthalate (PET) bottles are manufactured with the addition of plasticizers

[1)] Department of Chemistry, Faculty of Mathematics and Natural Sciences, University of Hasanuddin, Makassar, 90245 Indonesia.

[2)] Department of Biology, Faculty of Mathematics and Natural Sciences, University of Hasanuddin, Makassar, 90245 Indonesia.

[3)] Department of Environmental Engineering, Faculty of Engineering, University of Hasanuddin, Makassar, 90245 Indonesia.

[4)] Department of Chemistry, Faculty of Mathematics and Natural Sciences, University of Tanjungpura, Pontianak, 78124 Indonesia.

[*)] Author for correspondence: stfauziah@unhas.ac.id

such as di-(2-ethylhexyl) phthalate (DEHP), dibutylbenzyl phthalate (BBP), dibutyl phthalate (DBP), and diisononyl phthalate (DINP) [3]. Phthalate compounds such as DBP can dissolve in water [3, 4] and, when ingested, cause reproductive and endocrine disorders [5, 6], and DEHP is carcinogenic [7].

Especially, DBP is used as a plasticizer for various food product packaging, beverages [4], cosmetics, toys, and others that have the potential to interfere with human health. Therefore, it is necessary to analyze the existence of the DBP in various products. One of the methods used to determine DBP levels is solid phase extraction (SPE) [8] because this method is simple and selective [9]. The choice of proper adsorbent is important in the SPE method. Molecularly imprinted polymers (MIP) are the common choice of adsorbent in the SPE method for selective adsorption. [9, 10]. MIP has high affinity and selectivity against target molecules through its reusable active site [11], resistance to temperature, acid, and long shelf life [10]. MIPs is widely utilized in purification and extraction process [12] as well as chemical sensors [12, 13]. MIP morphology consists of cavities or pores that can adsorb target molecules [12]. MIP synthesis involves a monomer, crosslinker, initiator, template molecule, and pyrogen solvent [14, 15]. Methyl methacrylate (MMA) is widely used as a monomer because of its stability and hydrogen interactions between carbonyl functional groups with crosslinkers to form MIP [16]. MMA and crosslinkers (ethylene glycol dimethacrylate, EGDMA) affect the selectivity and maintain the morphology, stabilize the binding sites that have been formed, and maintain mechanical stability with the polymer matrix [15, 17].

An effective and frequently used polymerization method in the synthesis of MIP is precipitation [18]. Developments related to the MIP, research about synthesis and characterization of polymer imprinted with DEHP and DBP compounds as target molecules using MMA as monomer and TRIM using precipitation method need to be conducted.

The aim of the work was to synthesize unprinted polymers (NIP) and molecularly printed polymers (MIP). The resulting MIP were characterized using Fourier transform infrared (FTIR) spectroscopy, scanning electron microscopy (SEM), energy dispersive spectroscopy (EDS), surface area analysis (SAA), ultraviolet-visible spectrophotometry (UV-Vis). Moreover, their ability to adsorb DEHP and DBP compounds was determined.

EXPERIMENTAL PART

Materials

DEHP 99.5%, DBP 99.5%, methyl methacrylate (MMA) 99%, trimethylolpropane trimethacrylate (TRIM), and benzoyl peroxide (BPO) 75% were delivered from Sigma Aldrich, USA. Acetone, toluene, methanol, and acetic acid 96% were obtained from Merck, Germany.

Synthesis of NIP, MIP_DEHP, and MIP_DBP

To two round-bottom flasks containing 1 mM DEHP and DBP, respectively, 4 mM MMA with 8 mM TRIM as a crosslinker was added. Then 50 ml of toluene as a pyrogenic solvent were added and left for 10 min. In the next step, the solution was sonicated for 10 min and then nitrogen was purged for 10 min to remove oxygen. 1 mmol of BPO was added to the solution, sonicated and nitrogen purged again for 15 minutes. Polymerization was carried out by heating the solutions to 60°C for 24 h [19]. The obtained polymers (MIP_DEHP(BE) and MIP_DBP(BE)) were rinsed with acetone, methanol, and distilled water, respectively. DEHP and DBP were then extracted from MIP by sonication for 30 min using acetic acid: methanol (1:8 v/v) to obtain MIP_DBP(AE) [20]. Both extracts were analyzed using a UV spectrophotometer to check the presence of DEHP and DBP. The extraction was repeated until the absorbance value was close to or equal to zero, confirming the absence of extractable compounds. The MIP material was rinsed with methanol and distilled water until neutral pH was reached and then oven-dried to prepare it for further characterization. In the same way, non-printing polymers (NIP) were produced without the use of DEHP and DBP and without an extraction process, which were later called NIP.

Characterization

Fourier transform infrared spectroscopy

MIP and NIP were analyzed by Fourier transform infrared (FTIR) spectroscopy with Shimadzu IRPrestige-21 apparatus (Kyoto, Japan) uses a bright ceramic light source at a temperature of 28°C. The samples were analyzed with 300-second scans and resolution 4 at wavenumber between 3500 cm^{-1} to 350 cm^{-1}. The material is printed into plates using potassium bromide KBr with ratio sample and KBr (1:10) where 2 mg MIP sample were mixture with 20 mg KBr.

Scanning electron microscopy and energy dispersive spectroscopy (SEM-EDS)

The morphology and elements percentage were observed using a scanning electron microscope (JSM-6510, JEOL, Japan) and energy dispersive spectroscopy (EDS), respectively. A voltage of 10 kV and a magnification of 5000× were used. EDS measurements were performed using a current intensity of 1 nA, PHA T3 mode, real time 50.51 sec, lifetime 50 sec, idle time 1%, count rate 1349 cps and energy range 0–20 keV.

Surface area analysis (SAA)

The surface area of MIP_DEHP and MIP_DBP was determined using surface area analyzer (Nova 1200e, Quantachrome Instruments, Odelzhausen, Germany). The

volume and mean radius of MIP pores were determined by the Barrett-Joyner-Halenda (BJH) method, and the surface area by the Brunauer-Emmett-Teller (BET) method. Both methods used the principle of nitrogen adsorption. The sample density was 1 g/cm^3. The volume of warm free spaces was 10.77 cm^3 (MIP_DEHP) and 11.34 cm^3 (MIP_DBP), respectively, while the volume of cold free spaces was 30.86 cm^3 (MIP_DEHP) and 32.87 cm^3 (MIP_DBP), respectively.

Adsorption ability

30 mg of NIP, MIP_DEHP and MIP_DBP were transferred into vial with 5 mL of DEHP and 10 mgL^{-1} DB. Afterwards, the mixture was stirred for 60 min and filtered. Precipitate was analyzed using a spectrophotometer UV-Vis (Shimadzu UV-2600, Kyoto, Japan) at 264.6 nm wavelength. The DEHP and DBP amount adsorbed by MIP and NIP was calculated using equation (1).

$$Q_e = \frac{V(C_0 - C_e)}{m} \quad (1)$$

Where: Q_e – the amount adsorbed (mg/g), V – the volume of the solution (L), C_0 – the initial concentration of the solution (mg/L), C_e – the concentration of the solution after the adsorption process (mg/L), m – the mass of MIP used (g) [21].

The time effect on the adsorption ability of DEHP and DBP by MIP

A total of 5 mL of DEHP and DBP standard solutions of 10 mgL^{-1} and 30 mg MIP were put into each of the seven vials. Furthermore, the mixture was stirred with time variations of 10, 30, 60, 90, 120, 150, and 180 min. After the adsorption process, the solutions were filtered, and the filtrates were analyzed using spectrophotometer Shimadzu UV-2600 at 264.6 nm wavelength. Adsorption kinetics study was determined using kinetic models of pseudo-first order and pseudo-second order [22].

The concentration effect on adsorption ability of DEHP and DBP by MIP

A total of 5 mL of DEHP and DBP solutions at 5 different concentrations (6, 9, 12, 15, 18, 21, and 24 mg/L) were put in a vial containing 30 mg of MIP and stirred. Afterwards, the solution was filtered and analyzed using a spectrophotometer Shimadzu UV-2600 at 264.6 nm wavelength [20].

Determination of adsorption kinetics of MIP_DEHP and MIP_DBP

The adsorption kinetics of MIP_DEHP and MIP_DBP were determined from time effect analysis data using pseudo-first order and pseudo-second-order equations [23]. The pseudo-first-order equation is stated in equation (2), while the pseudo-second-order equation is expressed in equation (3).

$$\ln(Q_e - Q_t) = \ln(Q_e) - k_1 t \quad (2)$$

$$\frac{t}{Q_t} = \frac{1}{k_2 Q_e^2} + \frac{t}{Q_e} \quad (3)$$

Determination of adsorption capacity of MIP_DEHP and MIP_DBP

The adsorption capacities of MIP_DEHP and MIP_DBP were determined by analyzing the effect of concentration data using the Freundlich adsorption isothermal and Langmuir isotherms [24]. The Langmuir adsorption isothermal equation is stated in equation (2), while the Freundlich adsorption isothermal equation is expressed in equation (3).

RESULTS AND DISCUSSION

Synthesis of MIP_DEHP and MIP_DBP

MIP is a synthetic product of polymerization reactions of monomers, crosslinkers, and templates that interact via covalent or noncovalent bonds [25]. MIP_DEHP and MIP_DBP were synthesized by precipitation method using MMA monomer, TRIM crosslinker, and BPO initiator. The molecular structures of DEHP, DBP, MMA, TRIM, and BPO are shown in Figure 1.

MIP_DEHP and MIP_DBP are white powders. The DEHP and DBP compounds in MIP were washed sequentially with acetone, methanol, and distilled water by repeated sonication extraction to obtain polymers with imprinted MIP_DEHP$_{(AE)}$ and MIP_DBP$_{(AE)}$ molecules. DEHP and

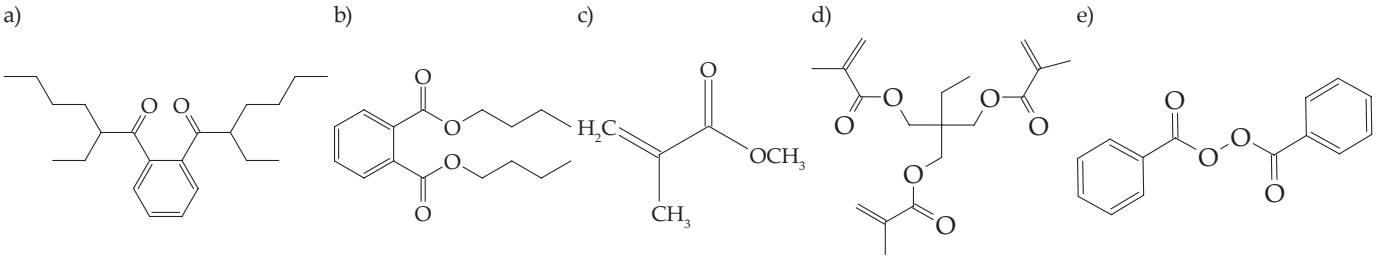

Fig. 1. Molecular structure: a) DEHP, b) DBP [26], c) MMA, d) TRIM [27], and e) BPO [27, 28]

T a b l e 1. UV-Vis results of DEHP and DBP compounds in a mixed solvent extract of methanol: acetic acid (8:2)

Extraction	Absorbance, a.u.	
	DEHP	DBP
Extract 1	4.29	4.43
Extract 2	3.95	4.29
Extract 3	3.18	2.52
Extract 4	1.92	1.53
Extract 5	1.29	1.28
Extract 6	0.91	0.92
Extract 7	0.63	0.67
Extract 8	0.33	0.39
Extract 9	0.13	0.20

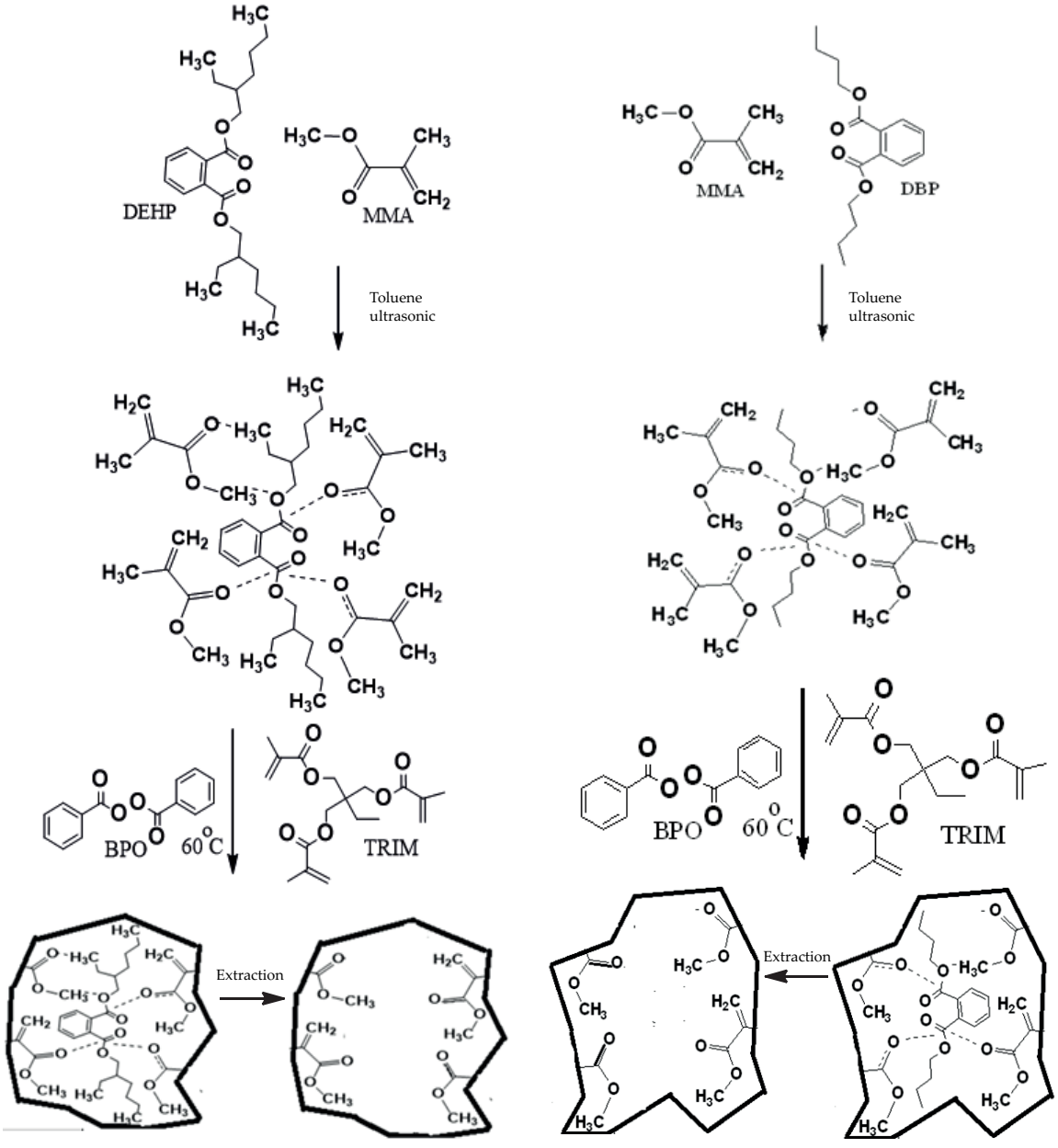

Fig. 2. Polymerization reaction of MIP_DEHP, and MIP_DBP extraction

T a b l e 2. FTIR analysis of MMA, NIP_MMA-co-TRIM, MIP_DEHP$_{(BE)}$ and MIP_DEHP$_{(AE)}$, MIP_DBP$_{(BE)}$ and MIP_DBP$_{(AE)}$ monomers

Functional groups	Wavenumber, cm^{-1}					
	MonomerMMA	NIP_MMA-co-TRIM	MIP_DEHP$_{(BE)}$	MIP_DEHP$_{(AE)}$	MIP_DBP$_{(BE)}$	MIP_DBP$_{(AE)}$
–CH stretching	2955	2957	2959	2957	2959	2956
–C–O stretching	1155	1153	1150	1152	1143	1152
–C=O stretching	1730	1734	1732	1730	1734	1732
–C=C stretching	1636	1641	1634	1634	1636	1636

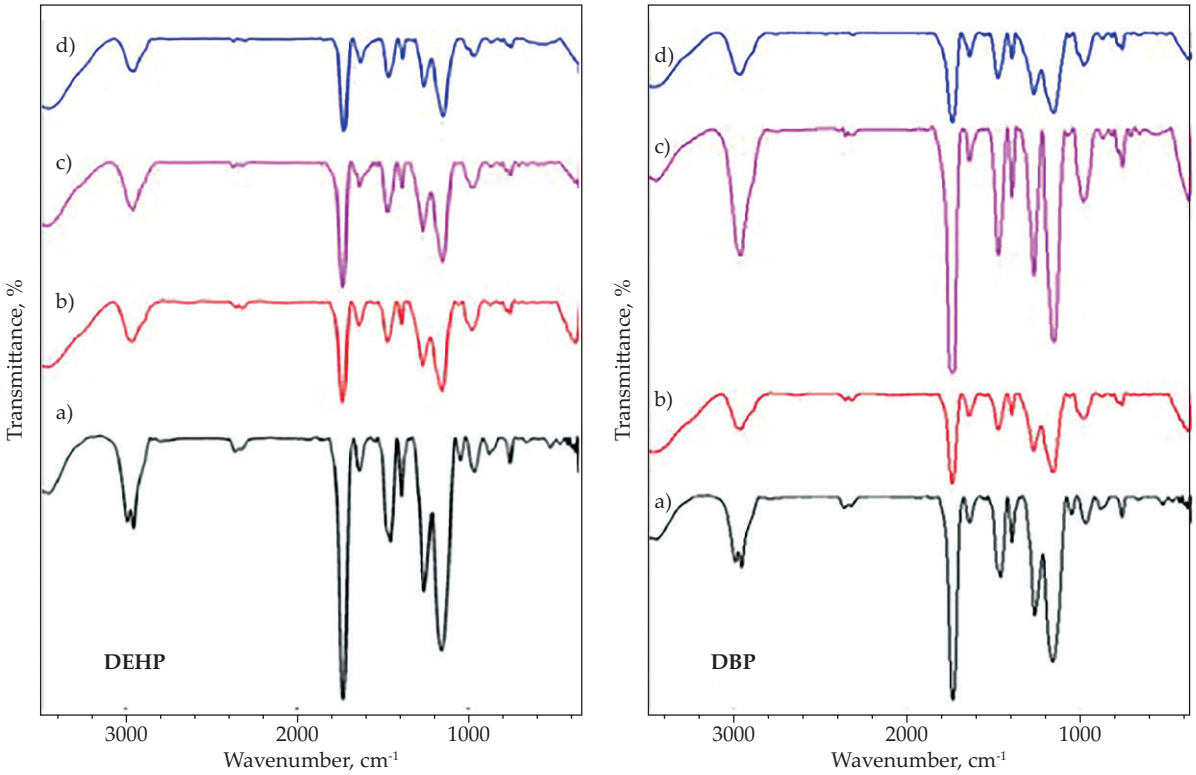

Fig. 3. FTIR spectra: a) MMA, b) NIP, c) MIP_DEHP$_{(BE)}$ and MIP_DBP$_{(BE)}$, d) MIP_DEHP$_{(AE)}$ and MIP_DBP$_{(AE)}$

DBP compounds extracted from MIP were detected by UV-Vis at 262.6 nm wavelength using a methanol: acetic acid (8:2 v/v) solution. The results are presented in Table 1.

The data in Table 1 show a decreasing absorbance value during subsequent extractions, confirming that DEPH and DBP were washed out of the MIP. The synthesis steps of MIP_DEHP and MIP_DBP consist of prepolymerization, polymerization, and release of DEHP and DBP from the MIP matrix [17, 18]. The polymerization and extraction reactions are presented in a modified Figure 2 [29, 30]. The release of DEHP and DBP from MIP leaves a template matching DEHP and DBP as target molecules. DEHP and DBP interact with MIP functional groups noncovalently due to size and shape compatibility.

FTIR analysis

FTIR analysis of NIP and MIP_DEHP $_{(BE)}$, MIP_DEHP $_{(AE)}$, MIP_DBP $_{(BE)}$ and MIP_DBP$_{(AE)}$ are presented in Table 2. Figure 3 shows the FTIR spectra of NIP_MMA-co-TRIM, MIP_DEHP$_{(BE)}$ and MIP_DEHP$_{(AE)}$.

Stretching vibrations of the CH bond occur in all materials with different intensity. The intensity of the C-H peak in MIP_DEHP$_{(BE)}$ and MIP_DBP$_{(BE)}$ was higher compared to MMA, MIP_DEHP$_{(AE)}$ and MIP_DBP$_{(AE)}$ because DEHP and DBP also contributed to the peak area. The peaks of the C=O and C-O groups have the same intensity. After the extraction of DEHP and DBP from MIP, the absorption intensity of -C-O, C=O decreased. The FTIR data also show a wavenumber shift in the –C–O functional group from MIP_DEHP$_{(BE)}$ to MIP_DEHP$_{(AE)}$ and from MIP_DBP$_{(BE)}$ to MIP_DBP$_{(AE)}$ due to dipole-dipole interactions between MMA and DEHP and DBP. Compounds with carbonyl functional groups, including MMA, DEHP, DBP and TRIM, are characterized by high –C=O absorption intensity in all materials in the wave number range of 1730 cm^{-1}. The –C=C functional groups present in NIP, MIP_DEHP(BE), MIP_DEHP(AE), MIP_DBP(BE) and MIP_

T a b l e 3. EDS data of NIP and MIP before and after extraction

MIP type	Element	Mass, %			Atom content, %		
		NIP	Before extraction	After extraction	NIP	Before extraction	After extraction
MIP_DEHP	C	77.85	75.59	74.73	82.40	80.49	79.93
	O	22.15	24.41	24.81	17.60	19.51	19.92
MIP_DBP	C	77.85	76.32	76.11	82.40	81.11	80.93
	O	22.15	23.68	23.89	17.60	18.89	19.07

T a b l e 4. SAA results of MIP_DEHP and MIP_DBP after extraction

Sample	Surface area, m^2/g	Total pore volume, cm^3/g	Pore radius, nm
$MIP\_DEHP_{(AE)}$	202.80	0.28	5.57
$MIP\_DBP_{(AE)}$	465.48	0.60	5.12

DBP(AE) show a slight shift in the wavenumber value. However, the –C=C intensity after polymerization was lower than that of the MMA because the initiator breaks the double bond in the free radical polymerization reaction between cross-linking agents and monomers. The FTIR spectrum shows the functional groups that contribute to the formation of NIP, MIP_DEHP and MIP_DBP are C-H, -C-O, -C=O and -C=C.

EDS analysis

The atomic components of the polymer are identified using EDS. NIP, $MIP\_DEHP_{(BE)}$, $MIP\_DEHP_{(AE)}$, $MIP\_DBP_{(BE)}$, and $MIP\_DBP_{(AE)}$ are composed of C, O, and H atoms, but only carbon and oxygen are shown due to the small contribution of hydrogen atoms. The mass and C atom content can be used to determine the reduction in atom content or mass of carbon and oxygen during the extraction of DEHP and DBP from MIP. Table 3 shows the EDS data.

The data from Table 3 show that the percentage of C in MIP decreases after extraction and that of O increases. However, these changes are minor. This can be explained by the small amount of DEHP and DBP used. The results show that the DEHP and DBP compounds are terminated in the MIP.

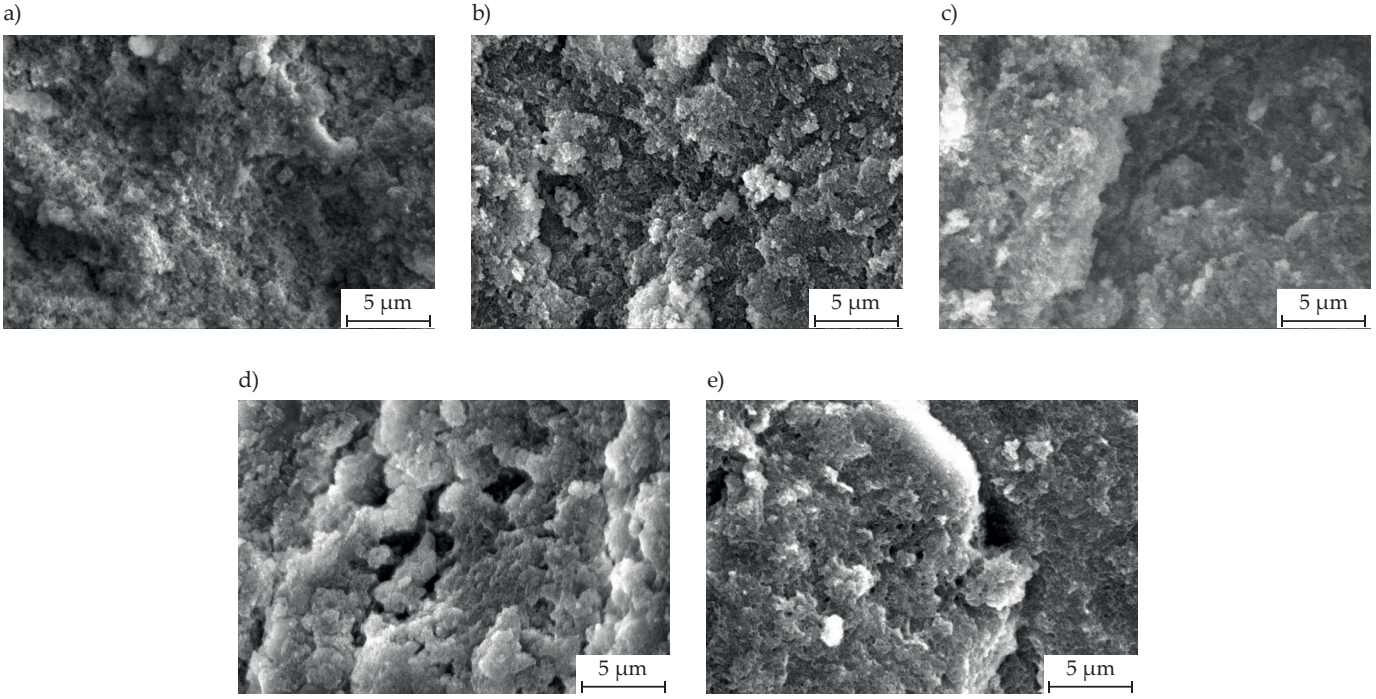

Fig. 4. SEM images at 5,000x magnification: a) NIP_MMA-co-TRIM, b) $MIP\_DEHP_{(BE)}$, c) $MIP\_DEHP_{(AE)}$, d) $MIP\_DBP_{(BE)}$, e) $MIP\_DBP_{(AE)}$

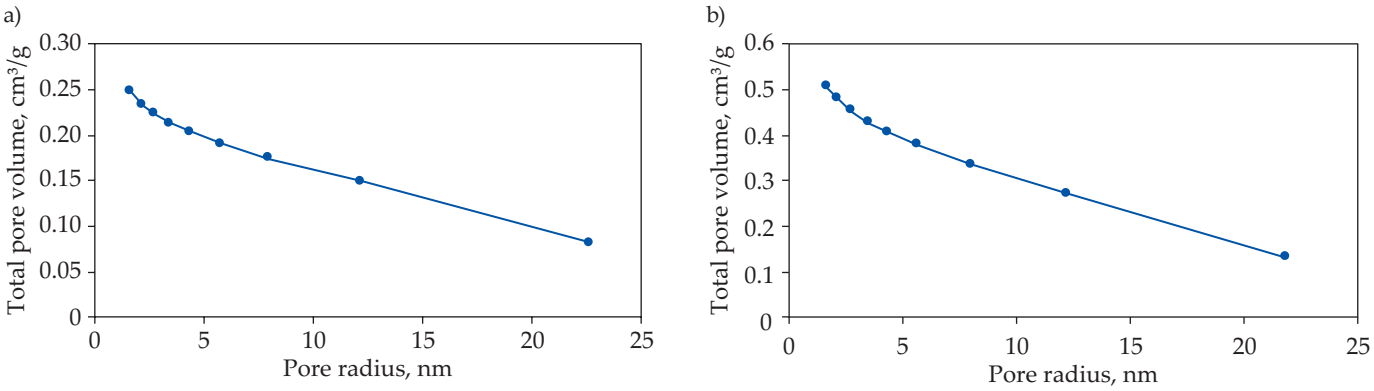

Fig. 5. The relationship between total pore volume and radius: a) MIP_DEHP$_{(AE)}$ and b) MIP_DBP$_{(AE)}$

SEM analysis

The results of surface morphological characterization of NIP_MMA-co-TRIM, MIP_DEHP$_{(BE)}$, and MIP_DEHP$_{(AE)}$, MIP_DBP$_{(BE)}$ and MIP_DBP$_{(AE)}$ can be seen in Figure 4. SEM images show small grains with different textures, densities, and sizes. NIP_MMA-co-TRIM is composed of small granules with a non-uniform and dense shape. MIP_DEHP$_{(BE)}$ is composed of tiny grains which tend to less dense and uniform in shape than NIP_MMA-co-TRIM. MIP_DEHP$_{(AE)}$ is the same as MIP_DEHP_MMA-co-TRIM$_{(BE)}$, but MIP_DEHP$_{(BE)}$ is thicker than MIP_DEHP$_{(AE)}$. The morphology of NIP_MMA-co-TRIM, MIP_DBP$_{(BE)}$, MIP_DBP$_{(AE)}$ is in the form of small round grains differing in size and density. The morphology of NIP_MMA-co-TRIM was composed of grains denser with shape and size are not uniform. Meanwhile, the morphology of MIP_DBP$_{(BE)}$ and MIP_DBP$_{(AE)}$ is composed of granules with a more uniform size. The surface morphology of MIP_DBP$_{(BE)}$ is more unified than MIP_DBP$_{(AE)}$.

Surface area analysis (SAA)

The surface area, total pore volume, and pore radius were determined by nitrogen adsorption-desorption analysis. The specific surface area of the polymer was evaluated using the Brunauer-Emmett-Teller (BET) method. In contrast, the pore volume and pore radius were assessed using the Barrett-Joyner-Halenda (BJH) method. Surface area, volume, and pore radius data can be seen in Table 4.

Table 4 shows that MIP_DEHP$_{(AE)}$ and MIP_DBP$_{(AE)}$ are mesoporous materials with the pore radius of 5.57 nm and 5.12 nm, respectively. The pore size classification according to IUPAC is micropores (pore radius < 2 nm), mesoporous (2 < pore radius < 50 nm), and macropores (pore radius > 50 nm). Other sizes based on N_2 adsorption at low pressure are mesopores (2–20 nm) and macropores (100–300 nm) [31]. In addition, MIP_DEHP$_{(AE)}$ and MIP_DBP$_{(AE)}$ has a surface area 203 and 465 m^2/g, respectively. The bigger the surface area of the polymer, the higher the adsorption capacity [32]. Figure 5 shows the BJH graphs of the pore distribution in MIP_DEHP$_{(AE)}$ and MIP_DBP$_{(AE)}$. The total pore volume of MIP_DEHP$_{(AE)}$ and MIP_DBP$_{(AE)}$ is 0.28 cm^3/g and 0.60 cm^3/g, respectively (Fig. 5).

The pore diameter range of MIP_DEHP$_{(AE)}$ is between 1.7 nm and 22.7 nm, where a diameter of pore size of 1.7 nm adsorbs N_2 of 0.25 cm^3/g and a diameter of 22.7 nm adsorbs N_2 gas of 0.08 cm^3/g. The pore diameter range of MIP_DBP$_{(AE)}$ is between 1.7 nm, and 21.9 nm, where diameter of pore size of 1.7 nm adsorbs N_2 of 0.51 cm^3/g and a diameter of 21.9 nm adsorbs N_2 gas of 0.13 cm^3/g. The adsorption of isothermal N_2 on MIP_DEHP$_{(AE)}$ can be seen in Figure 6. The blue curve expresses an increasing adsorption process whereas the relative pressure increases. In contrast, the red curve is a desorption process

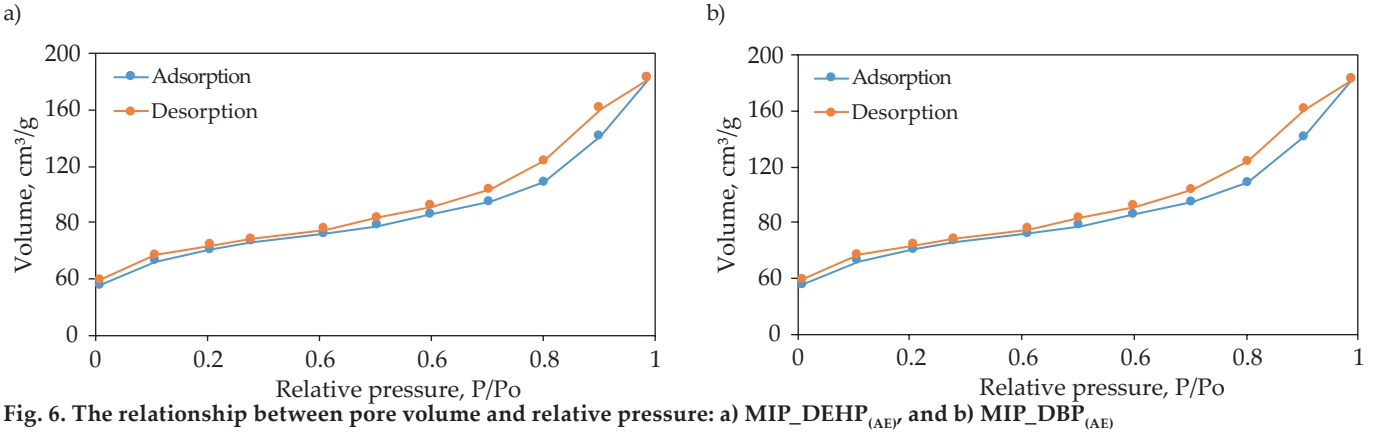

Fig. 6. The relationship between pore volume and relative pressure: a) MIP_DEHP$_{(AE)}$, and b) MIP_DBP$_{(AE)}$

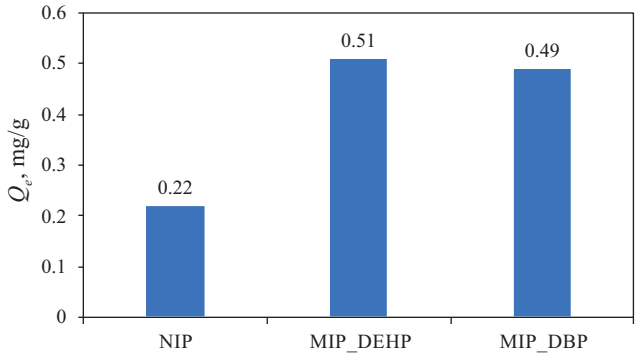

Fig. 7. Adsorption ability of NIP, MIP_DEHP, and MIP_DBP on DEHP and DBP

indicating a decrease in volume as the relative pressure decreases. MIP_DEHP$_{(AE)}$ and MIP_DBP$_{(AE)}$ can absorb N_2 gas as much as 182.65 cm^3/g and 385.18 cm^3/g respectively at 0.99 atm as a maximum pressure.

Adsorption ability

The adsorption ability of NIP, MIP_DEHP, and MIP_DBP for DEHP and DBP compounds can be seen compared to DEHP and DBP amount adsorbed by MIP in Figure 7.

MIP adsorbs DEHP and DBP better than NIP, where DEHP and DBP were adsorbed 0.29 mg/g and 0.20 mg/g, respectively, because the cavities formed in MIP_DEHP and MIP_DBP have the same shape and size as the DEHP and DBP compounds as target molecules. Therefore, MIP can adsorb better than NIP [22]. However, to determine the maximum adsorption ability, the MIP concentration and contact time must be optimized.

Effect of time on adsorption of DEHP and DBP by MIP

The effect of time on the adsorption capacity of DEHP and DBP by MIP was performed at different time intervals, as seen in Figure 8. The adsorption ability of MIP_DEHP$_{(AE)}$ and MIP_DBP$_{(AE)}$ initially increased and started to saturate at 90 minutes for MIP_DEHP$_{(AE)}$, where the adsorption capacity of the equilibrium MIP_DEHP$_{(AE)}$ was 0.37 mg/g and 150 minutes for MIP_DBP$_{(AE)}$ where the adsorption capacity the balance MIP_DEHP$_{(AE)}$ is 0.47 mg/g. The same thing happens with the effect of adsorption time on DBP by MIP_DBP_MAA-co-EGDMA after reaching the maximum adsorption and then reducing the adsorption capacity next time [33]. Time is an essential variable in determining the quality of MIP as an adsorbent. Therefore, the adsorption kinetics model is used to analyze the data to assess adsorption kinetics, including mass transfer and chemical reaction dynamics. Data on the effect of time on DEHP and DBP adsorption by MIP were analyzed using pseudo-first order and pseudo-second-order equations. The values of R^2, K_1 (apparent first-order kinetic constant), K_2 (pseudo-second-order kinetic constant), and Q_e from the calculation results and experimental results are shown in Table 5.

The adsorption kinetics can be determined by adjusting the adsorption data to various adsorption kinetic models. The data in Table 5 shows that DEHP adsorption by MIP_DEHP$_{(AE)}$ for the pseudo-second-order adsorption kinetics model (model 2) has a correlation coefficient (R^2) 0.99. The absorption ability (Q_e) calculated based on the pseudo second order kinetics model for MIP_DEHP$_{(AE)}$ is 0.33 mg/g, close to the experimental Q_e value, which

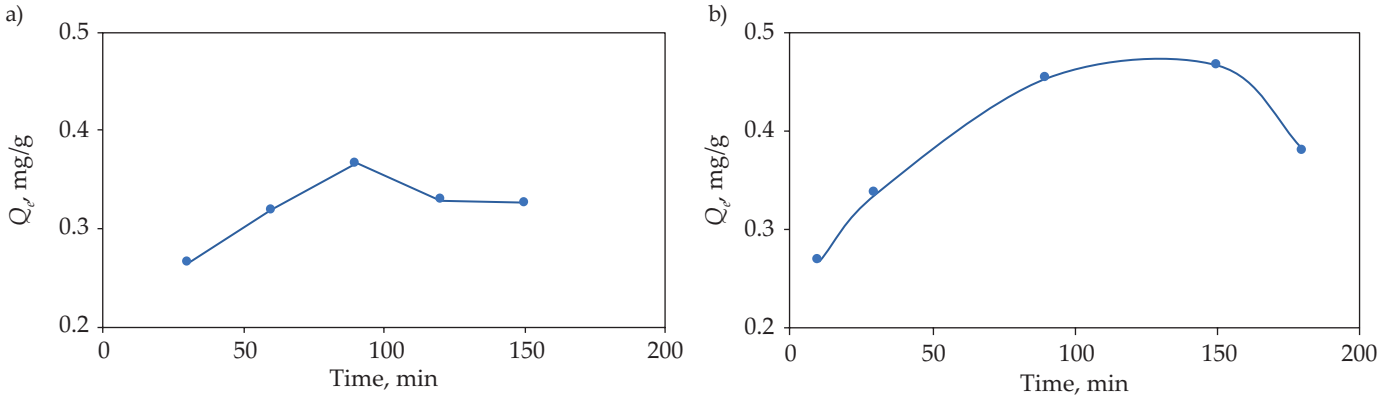

Fig. 8. Effect of time on the amount of: a) DEHP adsorbed by MIP_DEHP$_{(AE)}$, b) DBP adsorbed by and MIP_DBP$_{(AE)}$

T a b l e 5. Data of adsorption kinetics parameters of DEHP by MIP_DEHP$_{(AE)}$ and DBP by MIP_DBP$_{(AE)}$ based on pseudo-first order and pseudo-second-order kinetic equations

MIP type	Q_e, mg/g			Rate constant, g/mg · min		R^2	
	Model 1	Model 2	Experimental	K_1	K_2	Model 1	Model 2
MIP_DEHP$_{(AE)}$	0.26	0.33	0.37	-0.01	0.03	0.27	0.99
MIP_DBP$_{(AE)}$	0.17	0.42	0.47	-0.00	0.05	0.01	0.98

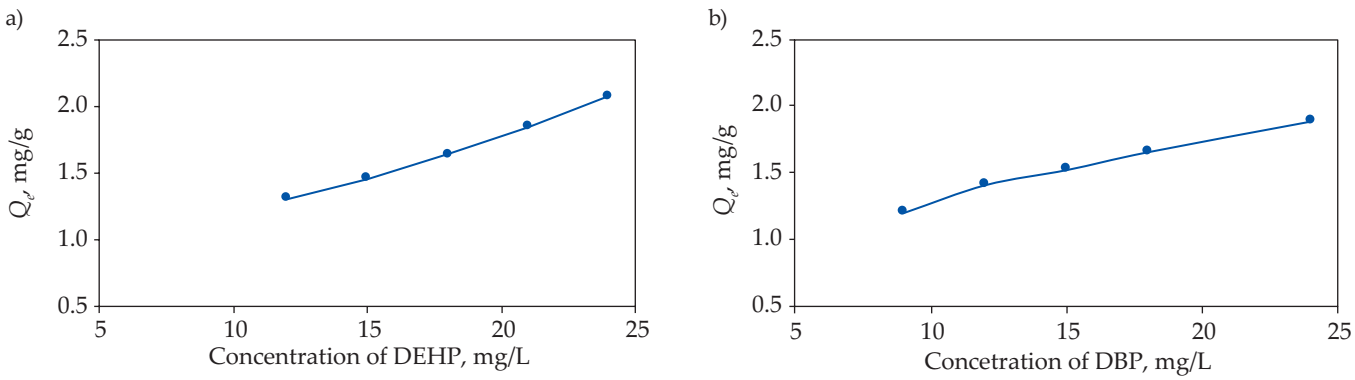

Fig. 9. The effect of concentration on the adsorption ability of: a) MIP_DEHP$_{(AE)}$ on DEHP, b) MIP_DBP$_{(AE)}$ on DBP

T a b l e 6. Adsorption parameters of DEHP by MIP_DEHP$_{(AE)}$ and DBP by MIP_DBP$_{(AE)}$ obtained from Langmuir adsorption isothermal and Freundlich adsorption isotherms

MIP type	Langmuir adsorption isotherm			Freundlich adsorption isotherm		
	K_L	q_m	R^2	K_F	n	R^2
MIP_DEHP$_{(AE)}$	0.22	2.69	0.91	0.68	2.27	0.95
MIP_DBP$_{(AE)}$	0.95	1.89	0.93	1.06	4.55	0.99

is 0.37 mg/g compared to the pseudo first-order kinetics model (model 1). The data obtained indicated that the MIP adsorption model synthesized in this study followed a pseudo-second-order adsorption kinetics model with an adsorption rate constant (K_2) MIP_DEHP$_{(AE)}$ of 0.03 g/min · mg.

The adsorption of DBP by MIP_DBP for the second-order adsorption kinetics model all has a correlation coefficient (R^2) closer to 1. The calculated Q_e value based on the pseudo second order kinetics model for MIP_DBP$_{(AE)}$ is 0.42 mg/g and is closer to the experimental Q_e value of 0.47 mg/g compared to the pseudo first order kinetics model. Based on the data obtained, it can be concluded that the MIP adsorption model synthesized in this study follows a pseudo-second-order adsorption kinetics model with an adsorption rate constant (K_2) MIP_DBP_MMA-co-TRIM$_{(AE)}$ of 0.05 g/min mg.

The effect of concentration on adsorption of DEHP by MIP_DEHP

The relationship between the amount of DEHP and DBP adsorbed by MIP and the concentration at equilibrium can be seen in Figure 9. The higher the initial concentration of the DEHP and DBP standard solutions, the more DEHP and DBP that can be adsorbed by MIP_DEHP$_{(AE)}$ and MIP_DBP$_{(AE)}$. However, if the adsorption equilibrium has reached the maximum limit, the adsorption capacity of MIP_DEHP$_{(AE)}$ and MIP_DBP$_{(AE)}$ will tend to remain the same even though the concentration is increased. The effect of concentration on the adsorption ability of MIP_DEHP$_{(AE)}$ on DEHP and MIP_DEHP$_{(AE)}$ on DBP can be seen in Figure 9.

The adsorption isothermal model fits the experimental data to predict the adsorption mechanism. MIP_DEHP$_{(AE)}$ and MIP_DBP$_{(AE)}$ adsorption capacities were determined using the Langmuir and Freundlich isothermal models. The appropriate adsorption isothermal model is determined from the linearity of the curve. The linearity of the Langmuir plot curve is obtained from the relationship $1/Q_e$ and $1/C_e$ in the Langmuir plot equation (equation 2). Meanwhile, the linearity of the Freundlich plot curve is obtained from the relationship between log Q_e and log C_e in the Freundlich plot (equation 3).

The Langmuir correlation coefficient values for MIP_DEHP$_{(AE)}$ and MIP_DBP$_{(AE)}$ are 0.91 and 0.93, respectively, while the Freundlich correlation coefficient values for MIP_DEHP$_{(AE)}$ and MIP_DBP$_{(AE)}$ individually are 0.95 and 0.99, respectively. The deviation of the data from the straight line in the Langmuir isotherm indicates that this model is incompatible with the adsorption mechanism. Therefore, the Freundlich adsorption isothermal model was used to determine the adsorption capacities of MIP_DEHP$_{(AE)}$ and MIP_DBP$_{(AE)}$. In general, the adsorption parameters of each isothermal model are presented in Table 6.

Table 6 shows the K_F values of MIP_DEHP$_{(AE)}$ and MIP_DBP$_{(AE)}$ were 0.68 mg/g and 1.06 mg/g, respectively, which illustrate the adsorption capacities of MIP_DEHP$_{(AE)}$ and MIP_DBP$_{(AE)}$. The adsorption intensities (n) of MIP_DEHP$_{(AE)}$ and MIP_DBP$_{(AE)}$ were 2.27 and 4.55, respectively. Values between 1-10 indicate highly effective absorption by MIP [34]. That is mean DEHP and DBP adsorption is quite effective by MIP_DEHP$_{(AE)}$ and MIP_DBP$_{(AE)}$. The 1/n value related to the adsorption strength on a heterogeneous surface, where < $1/n$ value indicates more significant expected heterogeneity. A $1/n$ value close to zero indicates a more heterogeneous adsorption surface, $1/n < 1$ indicates normal adsorption, whereas $1/n > 1$ indicates cooperative adsorption. The $1/n$ values obtained for MIP_DEHP$_{(AE)}$ and MIP_DBP$_{(AE)}$

were 0.44 and 0.22, respectively, indicating a more heterogeneous adsorption surface. The concordance of the Freundlich isotherm suggests that the adsorption occurs on the porous heterogeneous surface [16].

CONCLUSIONS

NIP, MIP_DEHP and MIP_DBP were successfully synthesized by precipitation polymerization. The FTIR spectra show characteristic peaks of C-H, -C-O, -C=O and -C=C functional groups, which indicates the formation of NIP, MIP_DEHP and MIP_DBP polymers. Small, uniform, and porous grains were observed in SEM micrographs. The EDS results showed a reduction in the percentage of C, indicating the formation of MIP_DEHP and MIP_DBP. The SAA results show that MIP_DEHP and MIP_DBP are mesoporous materials as the average pore radius is 5.57 nm and 5.12 nm, respectively. The total pore volume of MIP_DEHP and MIP_DBP was 0.28 and 0.6 cm^3/g, respectively. The surface area of MIP_DEHP was 203 m^2/g and MIP_DBP was 465 m^2/g. The adsorption kinetics models used are consistent with the pseudo-second-order adsorption kinetics model. The adsorption capacity of MIP_DEHP and MIP_DBP was 0.68 mg/g and 1.06 mg/g, respectively, according to the Freundlich isothermal adsorption model. MIP_DEHP and MIP_DBP are effective adsorbents of DEHP and DBP compounds and can be used as test materials for DEHP and DBP content in drinking water samples.

ACKNOWLEDGMENT

The authors thank Hasanuddin University for the financial support of the Hasanuddin University Collaborative Fundamental Grant program, Makassar, Indonesia (contract number 00323/UN4.22/PT.01.03/2023, January 25, 2023).

REFERENCES

[1] Luís C., Algarra M., Câmara J.S. *et al*.: *Toxics* **2021**, *9(7)*,157. https://doi.org/10.3390/toxics9070157
[2] Kumari A., Kaur R.: *PeerJ*. **2022**,10: e12859. https://doi.org/10.7717/peerj.12859
[3] Esteki F., Karimi H., Moazeni M. *et al*.: *Iran. Journal of food quality and hazards control* **2021**, *8(2)*, 66. https://doi.org/10.18502/jfqhc.8.2.6470
[4] Abdul R.H., Ungku Z.A.U.F., Jinap S. *et al*.: *Pertanika Journal of Tropical Agricultural Science* **2021**, *44(2)*, 389. https://doi.org/10.47836/pjtas.44.2.08
[5] Wang Y., Qian H.: *Healthcare (Basel)* **2021**, *9(5)*, 603. https://doi.org/10.3390/healthcare9050603
[6] Prevarić V., Bureš M.S., Cvetnić M. *et al*.: *Chemical and Biochemical Engineering Quaterly* **2021**, *35(2)*, 81. https://doi.org/10.15255/CABEQ.2021.1928
[7] Miao Y., Wang R., Lu C. *et al*.: *Environmental Science and Pollution Research* **2017,** *24*, 312. https://doi.org/10.1007/s11356-016-7797-4
[8] Zhang Z., Luo L., Cai R. *et al*.: *Biosensors and Bioelectronics*, **2013**, *49*, 367. https://doi.org/10.1016/j.bios.2013.05.054
[9] Yang Y., Yu J., Yin J. *et al*.: *Journal of Agricultural and Food Chemistry* **2014**, *62(46)*, 11130. https://doi.org/10.1021/jf5037933
[10] Vasapollo G., Sole R.D., Mergola L. *et al*.: *International Journal of Molecular Sciences*, **2011**, *12(9)*,5908. https://doi.org/10.3390/ijms12095908
[11] Hashemi-Moghaddam H., Rahimian M., Niromand B.: *Bulletin of the Korean Chemical Society* **2013**, *34(8)*, 2330. https://doi.org/10.5012/bkcs.2013.34.8.2330
[12] Yulianti E.S., Rahman S.F., Whulanza Y.: *Biosensors* **2022**, *12(12)*, 1090. https://doi.org/10.3390/bios12121090
[13] Beduk T., Gomes M., De Oliveira F.J.I. *et al*.: *Frontiers in Chemistry* **2022**, *10*:833899. https://doi.org/10.3389/fchem.2022.833899
[14] Kirsch N., Alexander C., Lubke M. *et al*.: *Polymer* **2000**, *14*, 5583. https://doi.org/10.1016/S0032-3861(99)00782-X
[15] Yan H., Row K.H.: *International Journal of Molecular Sciences* **2006**, *7(5)*, 155. https://doi.org/10.3390/i7050155
[16] Golker K., Karlsson B., Rosengren A. *et al*.: *International Journal of Molecular Sciences*, **2014**, *15(11)*, 20572. https://doi.org/10.3390/ijms151120572
[17] Hasanah A.N., Dwi U.T.N., Pratiwi R.: *Journal of Analytical Methods in Chemistry* **2019**, article ID 9853620. https://doi.org/10.1155/2019/9853620
[18] Hasanah A.N., Susanti I., Mutakin M.: *Molecules* **2022**, *27(9)*, 2880. https://doi.org/10.3390/molecules27092880
[19] Shahiri T.M, Rahnama K., Jahanshahi M. *et al*.: *Journal of Nanostructures* **2016**, *6(3)*, 245. https://doi.org/10.7508/JNS.2016.03.009
[20] Yang Z., Chen F., Tang Y. et al.: *Journal of the Chemical Society of Pakistan*, **2015**, *37(5)*, 939
[21] Zhou T., Tao Y., Jin H. *et al*: PLoS ONE **2016**, *11(1)*, Article ID e0147002. https://doi.org/10.1371/journal.pone.0147002
[22] Yusof N.A., Appribeyan M.D., Harson, J.: *Sains Malaysiana* **2010**, *39(5)*, 829.
[23] Dai C., Zhang J., Zhang Y. *et al*.: *Plos One* **2013**, *8(10)*, 1. https://doi.org/10.1371/journal.pone.0078167
[24] Ramakrishna D.M., and Viraraghavan T.: *Water, Air, and Soil Pollution* **2005**, *166(1)*, 49. https://doi.org/10.1007/s11270-005-8265-9
[25] Metwally M.G., Benhawy A.H., Khalifa R.M. *et al*.: *Molecules* **2021**, *26*, 6515. https://doi.org/10.3390/molecules26216515
[26] Zhan Y., Fangyan C., Yubin T. *et al*.: *Journal of the Chemical Society of Pakistan* **2015**, *37(5)*, 939.
[27] Hui Y., Hong-Bo L., Zhi-Shu T. *et al*.: *Journal of Environmental Chemical Engineering* 2021, *9(6)*, 106352.

https://doi.org/10.1016/j.jece.2021.106352
[28] Kusumkar V.V., Galamboš M., Viglašová E. *et al.*: *Materials* **2021**, *14*, 1083. https://doi.org/10.3390/ma14051083
[29] Shaikh H., Memon N., Khan H. et al.: *Journal of Chromatography A*. **2012,** *1247*, 125. https://doi.org/10.1016/j.chroma.2012.05.056
[30] Jin Y.F., Zhang Y.J., Zhang Y.P. *et al.*: *Journal of Chemistry*, **2013,** Article ID 903210. https://doi.org/10.1155/2013/903210
[31] Hu Li., Hongming T., and Majia Z.: *Minerals* **2019**, *9(9)*, 548. https://doi.org/10.3390/min9090548
[32] Chrisnandari R.D.: *Journal of Pharmacy and Science*, **2018**, *3(1)*. https://doi.org/10.53342/pharmasci.v3i1.74
[33] Fauziah S., Sullahi F.A., Soekamto N.H. *et al.*: *Asian Journal of Chemistry* **2021**, *33(4)*, 785. https://doi.org/10.14233/ajchem.2021.22992
[34] Febrianto J., Kosasih A.N., Sunarso J. *et al.*: *Journal of Hazardous Materials* **2009**, *162(2-3)*, 616. https://doi.org/10.1016/j.jhazmat.2008.06.042

Received 13 VI 2023